Z. Kristallogr. Suppl. **26** (2007) 593-598

Structures of magnesium and zinc long aliphatic chains carboxylates

A. Mesbah*, C. Juers, M. François, E. Rocca and J. Steinmetz

Laboratoire de Chimie du Solide Minéral Unité Mixte de Recherche N°7555
Université Henri Poincaré-Nancy I Faculté des sciences B.P. 239
F-54506 Vandoeuvre-lès-Nancy Cedex

Contact author; e-mail: adel.Mesbah@lcsm.uhp-nancy.fr.

Keywords: powder diffraction, synchrotron radiation, metallic soaps, polytypes.

Abstract. The crystallographic structures of metallic soaps acting as a barrier against aqueous corrosion, $Mg(C_{10}H_{19}O_2)_2(H_2O)_3$ **(MgC10)**, $Zn(C_{11}H_{21}O_2)_2$ **(ZnC11)**, $Zn(C_{12}H_{23}O_2)_2$ **(ZnC12)** and $Zn(C_{14}H_{27}O_2)_2$ **(ZnC14)** have been determined ab-initio from synchrotron powder diffraction data and refined by the Rietveld method. The structures are layered, the magnesium and zinc atoms being octahedraly and tetrahedraly O-coordinated in the sheets respectively. The zinc carboxylates present two various structures depending on the n value, the number of carbon in the aliphatic chains. Moreover, the powder patterns, for n constant, are complicated because of the presence of polytypes. Crystallochemistry of these metallic soaps is discussed.

Introduction

Electrochemical studies have shown that sodium linear monocarboxylate inhibits the corrosion of metal M (M = Mg, Fe, Cu, Zn, Pb) in aqueous solution. Particularly, the efficiency of these compounds with a general formula $CH_3(CH_2)_{n-2}COONa$ (n=7 to 18) is depending on the chain length of the aliphatic group. The metal passivation was attributed to the growth of a metallic soap $M(II)(CnH_{2n-1}O_2)_2(H_2O)_x$, called here MCn. A modelling of metal/$M(Cn)_2$ or metal oxidised/$M(Cn)_2$ interface should enable to understand, on an atomic scale, the mechanism of protection against corrosion of studied metals. It requires the knowledge of the crystallographic structures of the hydrophobic and protectives metal soaps. As they are relatively well crystallised, same structures of short or middle length chains carboxylates ($n \leq 10$) could be solved from single crystal data [1-3]. For the metal soaps with long aliphatic chains (n>10), single crystals suitable for diffraction analysis are more difficult to obtain. Thus, this paper deals with the structures of MgC10, ZnC11, ZnC12 and ZnC14 determined ab-initio from synchrotron powder diffraction data (the experiments were performed at LURE, ESRF and SLS).

Experimental

MgC10, ZnC10, ZnC12 and ZnC14 are prepared in aqueous solution following the reaction:

$$M(NO_3)_2 + 2(C_nH_{2n-1}O_2)Na + xH_2O \rightarrow M(C_nH_{2n-1}O_2)_2(H_2O)_x + 2Na^+ + 2\,NO_3^-.$$

Details of the procedure can be found elsewhere [1, 2].

XRPD and ab initio structure determination of MgC10, ZnC11, ZnC12 and ZnC14.

Data collection: X-ray powder diffraction data were collected by using different synchrotron radiation sources. The conditions of measurement for each sample are reported in Table 1: synchrotron source and beam line, geometry (transmission with capillary (Φ = 1 mm) or reflection on a flat plate sample), wave length, two-theta range, detection details. The capillary or flat sample rotates around the sample axis (phi-axis) or the normal to the sample surface. For avoiding radiation damage of the powdered metallic soap, the capillary was translated along the phi-axis to give a fresh region of sample every 15 mn (at ESRF) or a microstrip detector allowing one scan recording with less than one minute (at SLS) was used. In the last case at SLS, twenty scans were added for increasing the statistic.

Table 1:Experimental details of the synchrotron powder diffraction experiments

Compound	MgC10	ZnC11	ZnC12	ZnC14
Synchrotron source	ESRF (Grenoble, France)	LURE (Orsay, Paris)	SLS (villigen, Switzerland)	SLS (villigen, Switzerland)
Line	ID31[4]	WDIF4C [5]	X04SA [6]	X04SA [6]
Geometry	Transmission	Refection	Transmission	Transmission
Detection details	Nine crystals analyser Si(111)	One crystal analyser	Microstrip detector [7]	Microstrip detector [7]
Wave length (Å)	0.851243	0.69360	0.708838	0.708838
2θ range (deg)	0.021-32.96	2-40	1-30	1-30

ESRF: European Synchrotron Radiation facilities, SLS: Swiss Line Source, LURE: Laboratoire pour l'Utilisation du Rayonnement Electromagnétique.

Structure resolution: Standard peak search method with reflex from MSModeling program [8] was used to locate the diffraction maxima. X-Cell [9] was used for indexing the powder pattern. Localisation of the atoms was determined by ab initio methods in direct space using FOX program [10], the hydrogen atoms are not localised. Refinement of the four diagrams has been performed successively by the Pawley and Rietveld methods using FULLPROF_Suite software [11]. The crystal data and the structure refinement parameters are reported in Table 2. The Pawley refinements are satisfactory for the four compounds. The Rietveld refinement factors of MgC10 are satisfactory but not those of ZnC11, ZnC12 and ZnC14 which are relatively high (see Table 2). This is interpreted as being due to the existence of polytypes in the polycrystalline samples of zinc based compounds (see hereafter). The Rietveld refinement diagrams (observed, calculated and difference patterns) are represented in Figure 1a-d. The atomic coordinates have been deposited at the Cambridge Crystallographic Data Center, the CCDC reference numbers are indicated in Table 2.

Table 2: refinement data of MgC10, ZnC11, ZnC12 and ZnC14

Compound	**MgC10**	**ZnC11**	**ZnC12**	**ZnC14**
Formula	$Mg\ (C_{10}H_{19}O_2)_2.3\ (H_2O)$	$Zn\ (C_{11}H_{21}O_2)_2$	$Zn\ (C_{12}H_{23}O_2)_2$	$Zn\ (C_{14}H_{27}O_2)_2$
Fw(g.mol^{-1})	420.87	435.98	464.03	520.13
System	Monoclinic	Orthorhombic	Monoclinic	Monoclinic
Space group	P 2_1/a	Pna2_1	C2	C2
A (Å)	9.070(3)	9.337(1)	7.802(2)	7.785(1)
B (Å)	8.165(1)	4.738(4)	5.560(1)	5.538(1)
C (Å)	32.124(1)	54.630(1)	28.931(1)	33.211(7)
B (deg)	98.39(1)	/	90.67(2)	93.25(1)
V (Å^3)	2353.85(8)	2417.63(13)	1255.21(5)	1429.65(1)
Z	4	4	2	2
Dx (g.cm^{-3})	1.188	1.081	1.105	1.080
N obs of points	10982	6495	24827	24858
N_{ref}	808	1312	1741	1597
Pawley				
Rp	0.028	0.088	0.042	0.021
Rwp	0.042	0.124	0.070	0.039
χ^2	1.09	1.34	7.91	3.17
Rietveld				
Rp	0.037	0.197	0.074	0.050
Rwp	0.056	0.247	0.11	0.081
χ^2	2.05	5.08	33.2	23.2
R_{bragg}	0.069	0.247	0.210	0.210
CCDC code	600009	622015	622016	622017

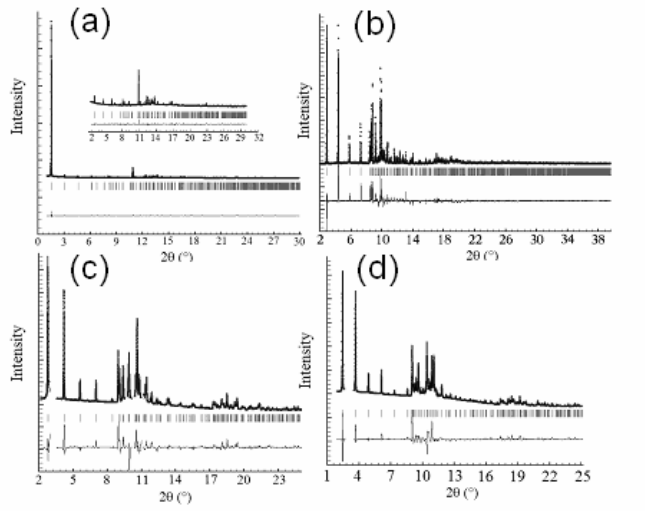

Figure 1. Rietveld refinement of a) MgC10, b) ZnC11, c) ZnC12 and d) ZnC14

Results and discussion

Structure description of MgC10

The structure of MgC10 is shown on *Figure 2.* The refinement led to the formula unit $Mg(C_{10}H_{19}O_2)_2.3(H_2O)$ showing that the compound is three-hydrated, in agreement with TGA results (not shown here). The structure is characterised by a lamellar stacking of sheets perpendicular to the longer axis c. The layers are centred by two plans of magnesium atoms parallel to (001). The structure contains two crystallographically independent chains named Ch1 and Ch2. The chains Ch1 and Ch2 are perpendicularly connected to each side of the metallic planes by the carboxylate groups. It should be emphasis that the aliphatic chains present some torsion angles differing of 180° in MgC10. The magnesium atoms have six O-coordinates in a deformed octahedral geometry, with distances Mg-O ranging between 2.09(2) and 2.15(3) Å.

The carboxylate group of the Ch1 chain is bidendate and bridging, i.e. the C-O bonds connect the adjacent octahedral units along the a axis. The carboxylate group of the Ch2 chain is monodendate. Thus the connection along b is performed by hydrogen bonds. The hydrogen bonds contribute to form the blocks constituting the basis of the layered structures, the layers being themselves linked by Van der Waals interaction between the $-CH_3$ terminal groups of the aliphatic chains.

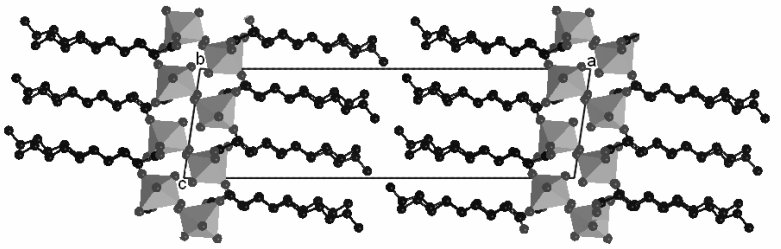

Figure 2. Structure of MgC10 projected along the b axis

Structures description of ZnC11, ZnC12 and ZnC14

General features: The structures of ZnC11, ZnC12 and ZnC14 are shown on the Figures 3 and 4. Contrarily to MgC10, they do not contain water molecules in agreement with TGA results (not shown here). The models presented here are noncentrosymmetric ($Pna2_1$ for ZnC11 and C2 for ZnC12, ZnC14). The structures are characterised by a lamellar stacking of polymeric sheets $[Zn(C_nH_{2n-1}O_2)_2]_n$ perpendicular to the longer axis (c axis). The sheets are linked by Van der Waals interactions. The layers are centred by a plan of zinc atoms parallel to (001). The "ZnO4" tetrahedrons are linked by bidendate and bridging carboxylates. Various orientations for "ZnO4" leading to **Type I** and **Type II** structures are found depending on the n value, the number of carbon atoms in the chains (see hereafter). The Zn-O distances range between 1.92(1) and 2.04(1) Å for Zinc carboxylates, and C-O distances between 1.27(1) and 1.29(1) Å. The C-C distances are around 1.50 Å.

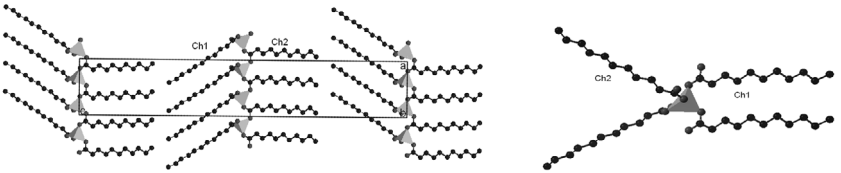

Figure 3. Structure of ZnC11 ($Pna2_1$) along b axis and the Zn tetrahedral environment showing the orientation of the linear undecanoate chains. ***Type I*** *structure.*

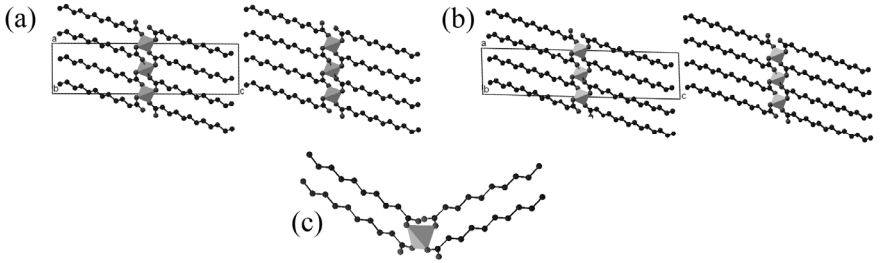

Figure 4. The Structure of a) ZnC12, b) ZnC14 projected along [010] and c) the Zn tetrahedral environment showing the orientation of the linear chains. ***Type II*** *structures.*

Detailed features: The structure of ZnC11 contains two crystallographically independent chains. The linear carboxylate chains named Ch1 are parallel while an angle of about 39.6° is made between the Ch2 chains as it is shown on the right of the Figure 3. The structures of ZnC12 (Fig. 4a) and ZnC14 (Fig. 4b) contain only one crystallographic independent chain. The tetrahedral O-environment for the zinc atoms and the orientation of the carboxylate chains, which differ from those of ZnC11, are represented on Figure 4c. The ZnC11 structure (**type I**) presents two alternating orientations for the 'ZnO4' tetrahedra (up and down) along the middle parameter (≈ 9.3 Å) which is twice the small parameter along which the tetrahedrons keep the same orientation. In the structures of ZnC12 and ZnC14 (**type II**), the tetrahedrons 'ZnO4' have the same orientation independently of the direction.

Based on the results presented here and previous results [1, 2] concerning zinc carboxylates with shorter aliphatic chains, a general law can be emphasis: For all $n < 10$ and for $n > 10$ with n odd, the structures adopt the **type I**. Basal lattice parameters are $b \approx 4.76$ Å and $a \approx 2$ x b. For $n \geq 10$ with n even, the structures adopt the **type II**. Basal lattice parameters are $a \approx 7.85$ Å, $b \approx 5.57$ Å.

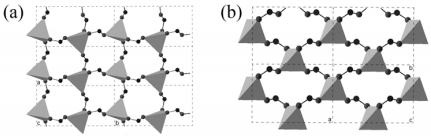

Figure 5: Representation of the Zn-tetrahedra linked by COO⁻ in a) 'Type I' and b) 'Type II' structures.

The presence of various polytypes in the zinc carboxylate samples makes the powder diagrams complicated and explains the high R value obtained from the Rietveld refinement of the structural models. The presence of polytypes has been proven for ZnC11 samples by the analysis of single crystals for which the space groups $P2_1/c$ (a = 54.460(4) Å, b = 4.670(4) Å, c = 9.240(8) Å and β = 92.47(1)°) and Cc (a = 53.451(2) Å, b = 4.670(4) Å, c = 9.178 (8) Å and β = 91.78(8)°) have been found. The related models are reported on Figure 6. The existence of polytypes is explained by the various ways of stacking the sheets linked by Van der Waals interactions. Conformational disorder or torsion of the aliphatic chains can also occur as it is shown on the Figure 6b.

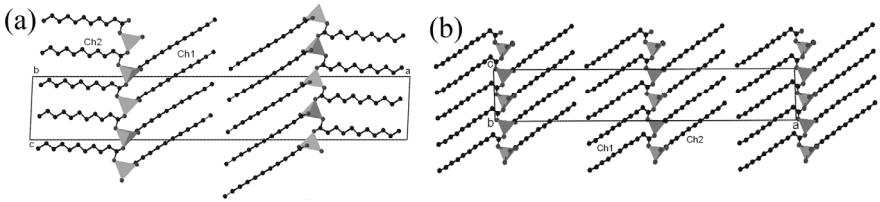

Figure 6. Structures of polytypes found in ZnC11 with a) P21/c and b) Cc space groups.

Conclusion

New structures have been determined ab initio methods in direct space for magnesium and zinc carboxylates from synchrotron powder data. While Rietveld refinement converges satisfactorily for magnesium carboxylate (MgC10), those of zinc carboxylates do not. It is explained by the presence of polytypes due to various possibilities of stacking the sheets. Efforts to improve the refinements by including several polytypes as it was observed on ZnC11 are in hand.

References

1. Peultier, J., François, M. & Steinmetz, J., 1999, *Acta Cryst.,* C**55**, 2064.
2. Lacouture, F., Peultier, J., François, M. & Steinmetz, J., 2000, *Acta Cryst.*, C**56**, 555.
3. Lacouture, F., François, M., Didierjean, C., Rivera, J-P., Rocca, E. & Steinmetz, J., 2001, *Acta Cryst.*, C**57**, 530.
4. Fitch, A.N., 2004, *J. Res. Natl. Inst. Stand. Technol.*, **109**, 133.
5. LURE W22 beam line. avaible from http://www.lure.u-psud.fr.
6. Swiss light source http://sls.web.psi.ch
7. Schmitt, B 2003, *physics research*, section A **501**, 267
8. http://www.accelrys.com/products/mstudio/modeling/
9. Neumann, M. , 2003, *J. Appl. Cryst.*, **36**, 356-365.
10. Favre-Nicolin, V. & Cerny, R., 2004, *Z. Kristallogr.*, **219** 847.
11. Rodriguez-Carvajal, J, FULLPROF version June 2005, ILL (unpublished).